

Halo Independent Direct Detection of Momentum-Dependent Dark Matter

John F. Cherry,¹ Mads T. Frandsen,² Ian M. Shoemaker²

¹Theoretical Division, Los Alamos National Laboratory, Los Alamos, New Mexico 87545, USA

²CP³-Origins and the Danish Institute for Advanced Study, University of Southern Denmark, Campusvej 55, DK-5230 Odense M, Denmark

Abstract.

We show that the momentum dependence of dark matter interactions with nuclei can be probed in direct detection experiments without knowledge of the dark matter velocity distribution. This is one of the few properties of DM microphysics that can be determined with direct detection alone, given a signal of dark matter in multiple direct detection experiments with different targets. Long-range interactions arising from the exchange of a light mediator are one example of momentum-dependent DM. For data produced from the exchange of a massless mediator we find for example that the mediator mass can be constrained to be $\lesssim 10$ MeV for DM in the 20-1000 GeV range in a halo-independent manner.

Preprint numbers: [LA-UR-14-23073](#), [CP3-Origins-2014-018](#) [DNRF90](#), [DIAS-2014-18](#)

Contents

1	Introduction	1
2	Direct Detection in v_{\min}-space	2
3	Momentum-Dependent Dark Matter Scattering in v_{\min}-space	3
4	Detector Mock-ups and Input Spectrum	5
5	Results	6
6	Conclusion	9
A	Signal Analysis	10
A.1	Basic χ^2 Test	10
A.2	Ratio Test	11

1 Introduction

A definitive, non-gravitational detection of Dark Matter (DM) has yet to occur. However a large number of low-background, direct searches for DM are underway with the goal of detecting the feeble nuclear recoil energy deposited by DM particles passing through the detector. The main target of these experiments are Weakly-Interacting Massive Particles (WIMPs), which are the most thoroughly studied DM candidates. The attractiveness of WIMP Dark Matter is driven by the fact that the relic abundance is controlled by their annihilation cross section. In the Early Universe, WIMPs are kept in thermal equilibrium by number-changing interactions, $\bar{X}X \leftrightarrow \bar{f}f$, where f is some SM particle. Eventually though, as the Universe expands and WIMPs are diluted, these number-changing interactions cease, and the abundance of WIMPs “freezes out.” Given that this paradigm requires DM to share some interactions with the SM, it provides many experimental lines of inquiry, and assuming that DM interacts with quarks or gluons it can be probed at direct detection experiments.

In view of the null results from direct detection and the LHC, simple models of thermal relic WIMPs termed Effective Field theory (EFT) models or ‘Maverick’ [1] models where the DM particle itself is the only new particle accessible at LHC, are nearly ruled out [2–4]. However, this conclusion is easily evaded when the EFT approach itself is not valid, as in the case of a mediator much lighter than the DM. Then annihilation of DM to a pair of mediators typically dominates over other available annihilation channels. In the case of asymmetric DM, the annihilation cross section requirement is even more stringent because one needs to “annihilate away” the symmetric abundance. Thus a light mediator coupling to DM remains a viable venue for symmetric or asymmetric DM.

In contrast with high-energy colliders, direct detection offers a sensitive probe of such light mediators at the cost of relying on the galactic DM halo to provide collisional energy. As a consequence of this direct detection experiments suffer from some uncertainty in the astrophysical distribution of DM. To combat this uncertainty, direct detection analysis using astrophysics-independent methods for interpreting data has gained increased interest recently [5–10].

In the present paper, we illustrate the utility of these methods in determining the momentum-dependence of the DM scattering and outline a new method which is also agnostic with respect to the velocity distribution of DM in the halo. Using this simple method, we perform a projection study of what up-coming ton-scale experiments can say about the presence of light mediators, and more generally momentum dependence of the scattering cross section. Similar projections have been recently made for momentum-independent cross sections [11, 12] and momentum-dependent cross sections [13] assuming specific models of the DM velocity distribution.

2 Direct Detection in v_{\min} -space

Direct detection involves a combination of dark matter particle physics, nuclear physics and astrophysics. It has been pointed out that in the case of simple spin-independent interactions, one can “integrate out” the DM astrophysics and compare experiments without any assumptions about the unknown local DM distribution [6, 14]. These methods have since been extended to cover momentum-dependent [8] and inelastic scattering [15].

For elastic, spin independent scattering, the differential event rate of scatters at a direct detection experiment is given by

$$\frac{dR}{dE_R} = \frac{1}{2\mu_{nX}^2} \left[\frac{f_p}{f_n} Z + (A - Z) \right]^2 F^2(E_R) \tilde{g}(v_{\min}), \quad (2.1)$$

where

$$\tilde{g}(v_{\min}) = \frac{\rho\sigma_n}{m_X} \int_{v_{\min}(E_R)}^{\infty} \frac{f(v + v_E(t))}{v} d^3v, \quad (2.2)$$

with σ_n the DM-neutron scattering cross section, m_X is the dark matter mass, $F(E_R)$ is the nuclear form factor, μ_{nX} is the nucleon-DM reduced mass, f_p/f_n is the ratio of the effective proton and neutron couplings to DM [16]. Finally $f(v + v_E(t))$ is the local DM velocity distribution evaluated in the galactic rest frame and $v_E(t)$ is the velocity of the Earth relative to the galactic rest frame.

The minimum velocity for an incoming DM particle to produce a nuclear recoil of energy E_R is

$$v_{\min}(E_R) = \sqrt{m_N E_R / 2\mu^2} \quad (2.3)$$

with μ being the DM-nucleus reduced mass. Lastly we also have in the above the astrophysics parameters ρ and $f(v)$ describing the local DM mass density and velocity distribution respectively. There is considerable uncertainty on these astrophysics parameters, and the DM inferences (e.g. its mass and scattering cross section) one naïvely draws from direct detection depend sensitively on their values.

Rather than assuming the values of ρ and $f(v)$, we can instead report halo independent constraints or parameter estimations on the quantities m_X , v_{\min} , and $\tilde{g}(v_{\min})$. Thus for example, for each fixed DM mass m_X we can simply use the observed rate dR/dE_R to infer $\tilde{g}(v_{\min})$ as a function of v_{\min} :

$$\tilde{g}(v_{\min}) = \frac{2\mu_{nX}^2}{[f_p/f_n Z + (A - Z)]^2 F^2(E_R)} \frac{dR}{dE_R}. \quad (2.4)$$

In performing such a mapping to v_{\min} -space in this way, we have assumed that the only momentum dependence in the scattering is in the nuclear form factor, where the relation between momentum transfer q and recoil energy is given by $q = \sqrt{2m_N E_R}$.

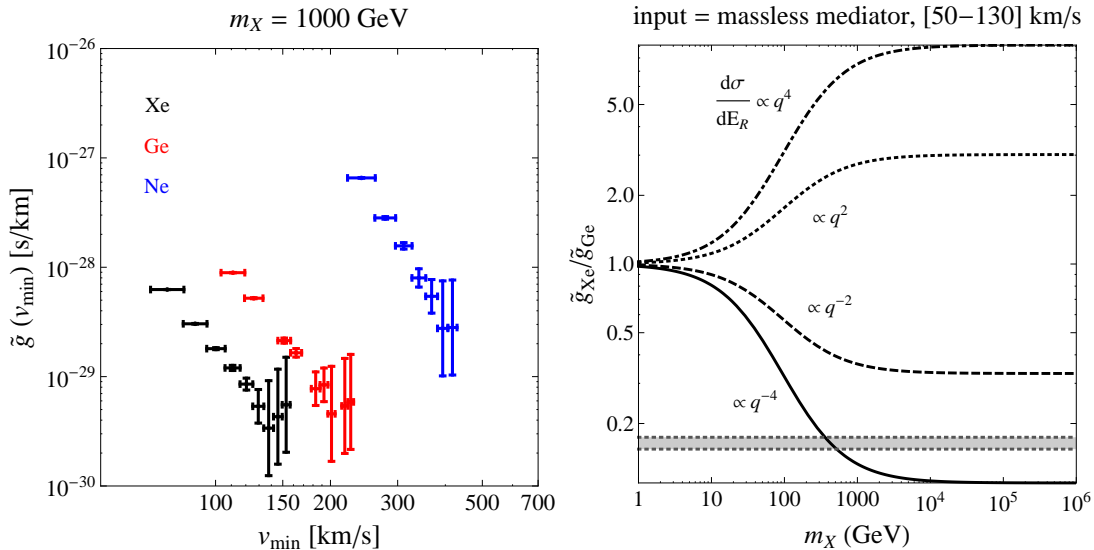


Figure 1. *Left:* Naively mapped event rates to $(\tilde{g} - v_{min})$ space with DM-nucleus scattering via a massless mediator. *Right:* Expected \tilde{g} ratio between a Xe and Ge target in which DM scattering has a non-trivial momentum-dependence, parameterised by the integer n as shown in Eq. (2.4). The observed \tilde{g} ratio in a $[50 - 130]$ km/s bin is the shaded band.

3 Momentum-Dependent Dark Matter Scattering in v_{min} -space

Let us now illustrate how a straightforward extension of this method can be used to extract information about the momentum dependence from direct detection data without making assumptions about the DM astrophysics.

Above in Eq.(2.4) we assumed that the energy-dependence from the DM microphysics is trivial, i.e. all the energy dependence is encoded in the nuclear form factor $F(E_R)$. There are many ways in which this assumption can be violated. An especially simple example, is that DM may exchange a very light mediator with nuclei. In this case, the cross section will scale as $d\sigma/dE_R \propto q^{-4}$. A simple parameterization [17] of non-trivial momentum-dependence is

$$\frac{d\sigma}{dE_R} = \left(\frac{d\sigma}{dE_R} \right)_0 \left(\frac{q^2}{q_{ref}^2} \right)^n \left(\frac{q_{ref}^2 + m_\phi^2}{q^2 + m_\phi^2} \right)^2, \quad (3.1)$$

where m_ϕ is the mass of the exchanged mediator, and we fix $q_{ref} = 10$ MeV throughout. Above, $(d\sigma/dE_R)_0$ is the standard spin-independent DM-nucleus cross section

$$\left(\frac{d\sigma}{dE_R} \right)_0 = \frac{m_N}{2\mu_{nX}^2 v^2} \sigma_n F^2(E_R). \quad (3.2)$$

Written in this way, the integer n parameterizes the unknown Lorentz structure of the DM-quark operator, while the momentum dependence from the propagator is explicitly factored out. Thus the standard spin-independent contact interaction scattering corresponds to the $n = 0$, heavy mediator limit $m_\phi^2 \gg q^2$. Note that the momentum transfer q is related to v_{min} as $q = 2\mu v_{min}$.

This can be seen illustrated in Figure 1. Working from an EFT framework, the data from all of the experiments with different target nuclei ought to agree on the shape of the

$\tilde{g}(v_{min})$ curve. This is clearly not the case and the strong tension between the different experiments is apparent to the eye. These data have been generated from a DM interaction which is carried by a massless mediator. This simple change alters the momentum dependence of the cross section to be $\propto q^{-4}$, mimicking what would otherwise be interpreted as a disagreement between experiments on the velocity distribution and density of the galactic DM halo. However, it is important to note that when the problem is approached carefully the compatibility of different experiments can be assessed independently DM astrophysics.

With the simple cross section parameterization in Eq. 3.1 we are at first interested in distinguishing two possibilities: the presence or absence of momentum dependence in the DM interaction. To answer this question, we can simply use Eq. 3.1 with $m_\phi \gg q, q_{ref}$, such that the cross section becomes

$$\frac{d\sigma}{dE_R} = \left(\frac{d\sigma}{dE_R} \right)_0 \left(\frac{q^2}{q_{ref}^2} \right)^n. \quad (3.3)$$

In this case the signal of non-trivial momentum dependence corresponds to $n \neq 0$.

We now imagine the fortunate situation where two experiments employing different target materials observe a signal. If the dark matter microphysics are momentum-dependent, the data will lead to discrepant inferences of $\tilde{g}(v_{min})$ under the assumption of Eq. (2.4). Suppose experiment i uses a target nucleus of mass m_{N_i} , $i = 1, 2$. With the signal spectrum produced from scattering of the type in Eq. (3.3), we expect experiment i to infer a value for $\tilde{g}(v_{min})$ of

$$\tilde{g}_{infer,i} = \tilde{g}_{true} \left(\frac{q^2}{q_{ref}^2} \right)^n = \tilde{g}_{true} \left(\frac{2\mu_i v_{min}}{q_{ref}} \right)^{2n} \quad (3.4)$$

where $\mu_i = m_X m_{N_i} / (m_X + m_{N_i})$. Taking the ratio of the inferred value of $\tilde{g}(v_{min})$ at the same v_{min} by two different experiments we obtain

$$\left. \frac{\tilde{g}_{infer,1}}{\tilde{g}_{infer,2}} \right|_{v_{min}} = \left(\frac{\mu_1}{\mu_2} \right)^{2n}. \quad (3.5)$$

At DM masses $m_X \gg m_{N_i}$ where $\mu_i \simeq m_{N_i}$, we expect a significant discrepancy to appear, implying momentum dependence of the true scattering cross-section. Instead at low DM masses $m_X \ll m_{N_i}$ when $\mu_i \simeq m_X$ and the momentum transfer is nearly identical for different targets, we expect little difference in the inferred values of \tilde{g} for different experiments and it will not be possible to distinguish between the above scenarios, e.g. [18].

We illustrate this in Fig. 1, where we plot the ratio of the inferred values of $\tilde{g}(v_{min})$ in Xenon, Germanium, and Neon experiments, using $m_X = 1000$ GeV, $m_\phi = 0$, Eq. (3.1), and assuming Helm nuclear form factors. Thus at each value of v_{min} that is compared, one expects an offset in the inferred value of \tilde{g} . The right hand panel of Fig. 1 illustrates the DM mass dependence of this offset, confirming that so long as we are not in the regime where $m_X \ll m_{N_i}$ momentum will produce an offset.

This simple \tilde{g} ratio diagnostic is easily extended to include the mediator mass dependence by using Eq. (3.1) such that Eq.(3.5) generalizes to

$$\left. \frac{\tilde{g}_{infer,1}}{\tilde{g}_{infer,2}} \right|_{v_{min}} = \left(\frac{\mu_1}{\mu_2} \right)^{2n} \left(\frac{\mu_2^2 + (m_\phi/v_{min})^2}{\mu_1^2 + (m_\phi/v_{min})^2} \right)^2. \quad (3.6)$$

Our strategy for determining the momentum dependence of the dark matter scattering is therefore to map the experimental data on dR/dE_R into bins in v_{min} space and compare

overlapping bins. In general, this mapping will be different for distinct experiments with different target nuclei and isotopic abundances, and will also depend on the hypothetical DM mass which we wish to test. This provides the benefit that our uncertainties of the velocity distribution of the DM in the galactic halo are guaranteed to cancel away when taking a ratio of two independent measurements. So long as the DM possesses a single velocity distribution, the distinct experiments are guaranteed to sample precisely the same portion of the $\tilde{g}(v_{min})$ curve. This provides a measurement of the DM interaction physics regardless of the de-facto shape of $\tilde{g}(v_{min})$, provided that m_X is not so light that the DM-Nucleus reduced masses of all experiments are degenerate. In the case where no bins overlap we can, in principle, extrapolate a best fit curve of $\tilde{g}(v_{min})$ through the available bins and then compare the inferred \tilde{g}_{vmin} functions. However this re-introduces dependence on the velocity function by way of forcing an observer to assume that the velocity distribution of the DM in the galactic halo corresponds to a known class of analytic functions (e.g. the Standard Halo Model) and the associated observational uncertainties.

Since we are interested in extracting the dependence of the cross-section on the momentum transfer, or equivalently the recoil energy, it is important to know the momentum dependence inherent in the nucleon and nuclear form factors. A general momentum dependence of the differential dark matter-nucleus scattering on a given nucleide per unit time and detector mass, assuming a single DM species, may be written as [19]

$$\frac{dR}{dE_R} = \frac{\kappa_X \rho}{m_X} \int_0^\infty \left[\sum_i (f_p^i(q, v) F_p^i(q, v) Z + (A - Z) f_n^i(q, v)) F_n^i(q, v) - T_2(q, v) \right]^2 \frac{f(v + v_E(t))}{v} d^3v, \quad (3.5)$$

where κ_X is a factor specific to the nature of the DM particle, i runs over the exchanged mediators and we include both separate nuclear form factors $F_{n,p}^i(q, v)$ for protons and neutrons and a form factor for two nucleon interactions $T_2(q, v)$ [19, 20] in addition to the single nucleon form factors $f_{p,n}^i(q, v)$. We also imagine a separation of $f_p^i(q) = f_{p,X}^i(q) f_{p,N}^i(q)$ where the first factor gives the particle physics momentum dependence of the interaction, arising from the DM-mediator vertex while the second factor gives the nuclear physics form factor. Thus in our example above in Eq. (3.1) we have assumed $f_{p,X}^i(q) = f_{n,X}^i(q) \sim q^{2n}$, $f_{p,N}^i(q) = f_{p,N}^i$, $T_2(q, v) = 0$ and an appropriate nuclear form factor $F_n^i(q, v) = F_p^i(q, v) = F(E_R)$.

For a scalar mediator, interacting with DM and quarks via Yukawa couplings with zero tree-level momentum dependence, the momentum dependent part of $f_{n,p}(q)$ and the $T_2(q, v)$ gives corrections to the rate of the order of a few percent below 100 keV nuclear recoil energies [19, 20]. The same is true for the momentum dependence of the Helm form factor $F(E_R)$ and more importantly we expect differences between the Helm form factor (included in the analysis) and a more accurate form factor are not above this level. Extracting the momentum dependence from DM particle physics is therefore feasible.

We provide the details of our analysis below, and a complete description of our techniques in Appendix A.

4 Detector Mock-ups and Input Spectrum

To reasonably well simulate the near-term experimental capabilities, we include efficiencies, energy resolution, exposures, and background expectations. Similar theoretical projections

target	ϵ_{eff} [ton \times yr]	E_{thr} [keV]	$\sigma(E)$ [keV]
Xe	0.88	5	$0.6 \text{ keV} \sqrt{E_R/\text{keV}}$
Ge	0.88	5	$0.5 \text{ keV} \sqrt{(0.3)^2 + (0.06)^2 E_R/\text{keV}}$
Ne	0.88	5	$1 \text{ keV} \sqrt{E_R/\text{keV}}$

Table 1. Characteristics of future direct dark matter experiments using Xenon, Germanium and Neon as target nuclei.

have been made previously with momentum-independent [11, 12] and momentum-dependent cross sections [13] assuming specific models of the DM velocity distribution.

The Gaussian energy resolution for each target is specified in Table 1. The number of events expected in the energy range $[E_1, E_2]$ is:

$$N(E_1, E_2) = \text{Exp} \int \text{Res}(E_1, E_2, E_R) \epsilon(E_R) \frac{dR}{dE_R} dE_R, \quad (4.1)$$

where Exp is the raw exposure (not including detector/analysis cut efficiencies), and $\text{Res}(E_1, E_2, E_R)$ is the detector response function taken to be

$$\text{Res}(E_1, E_2, E_R) = \frac{1}{2} \left[\text{erf} \left(\frac{E_2 - E_R}{\sqrt{2}\sigma(E_R)} \right) - \text{erf} \left(\frac{E_1 - E_R}{\sqrt{2}\sigma(E_R)} \right) \right]. \quad (4.2)$$

We assume that the each mock experiment will achieve their stated goals of reaching a < 1 background event expectation.

Though the velocity distribution remains unknown it has become canonical to assume a Maxwell-Boltzmann (MB) distribution [21, 22], truncated at the escape speed. We use this standard halo model (SHM) as our fiducial $f(v)$ choice to generate mock experimental spectra and note that detailed simulations of DM structure formation do not appear to deviate markedly from this choice [23].

In the rest frame of the Milky Way the velocity distribution,

$$f_{MB}(\vec{v}) = \begin{cases} N e^{-v^2/v_0^2}, & v < v_{esc} \\ 0, & v > v_{esc} \end{cases}, \quad (4.3)$$

is determined by its dispersion v_0 and the local escape speed v_{esc} . In this case the velocity integral $g(v_{min})$ corresponding to the SHM has a closed form expression [16, 24–26].

In the SHM the dispersion is equated to the circular speed which is observable and measured to be $\langle v_c(t) \rangle = 230 \text{ km/s}$ [27, 28]. We use a local DM density $\rho_{DM} = 0.3 \text{ GeVcm}^{-3}$ and escape speed $v_{esc} = 550 \text{ km/s}$.

5 Results

To generate our mock signals, we have taken representative points in parameter space consistent with the LUX null results [29]. The details of our LUX treatment can be found in [20, 30, 31]. Fits to the individual data sets for each detector medium are performed with standard χ^2 plus Log Likelihood analysis, which in addition to fitting n , m_ϕ , and m_X optimizes the best fit in the velocity dispersion, σ_v , of the SHM. The individual datasets are then combined into a master dataset where the same χ^2 plus Log Likelihood analysis is performed for a “global” analysis. The details of this analysis can be found in A.1. Once these tests are complete, the \tilde{g} ratio test is also conducted on the original data set for every v_{min} bin in

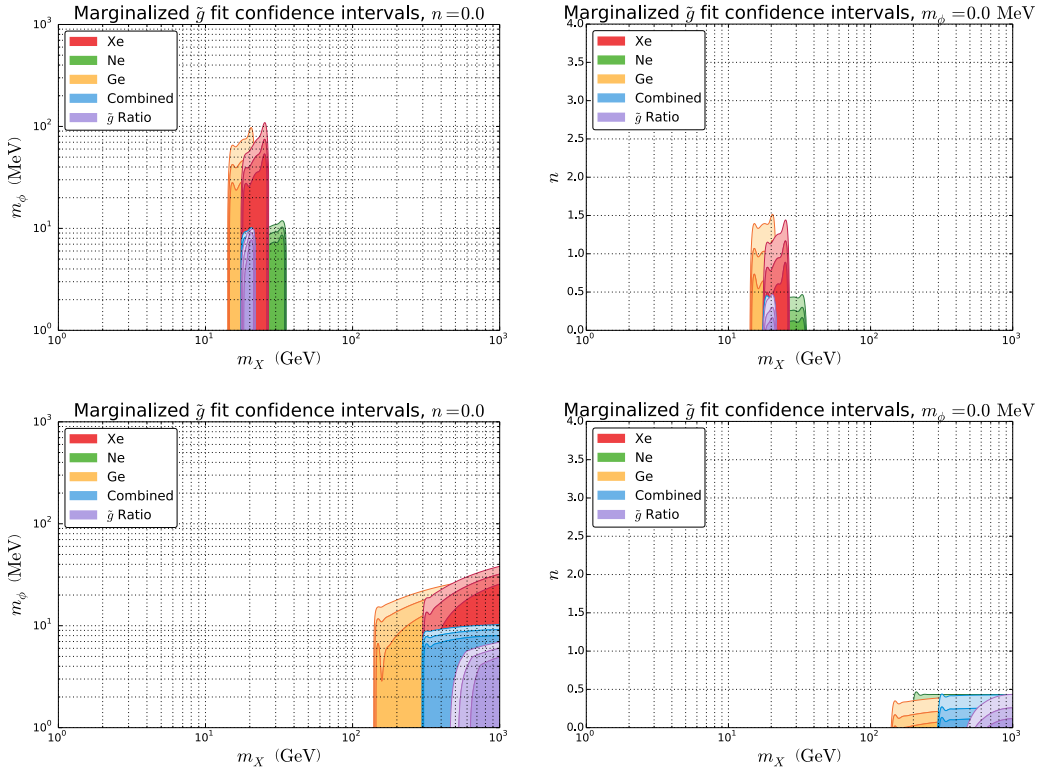


Figure 2. Reconstruction of DM parameters from an input spectrum generated via a massless mediator. The results on the first row correspond to DM mass $m_X = 20$ GeV, and the bottom row to 1000 GeV.

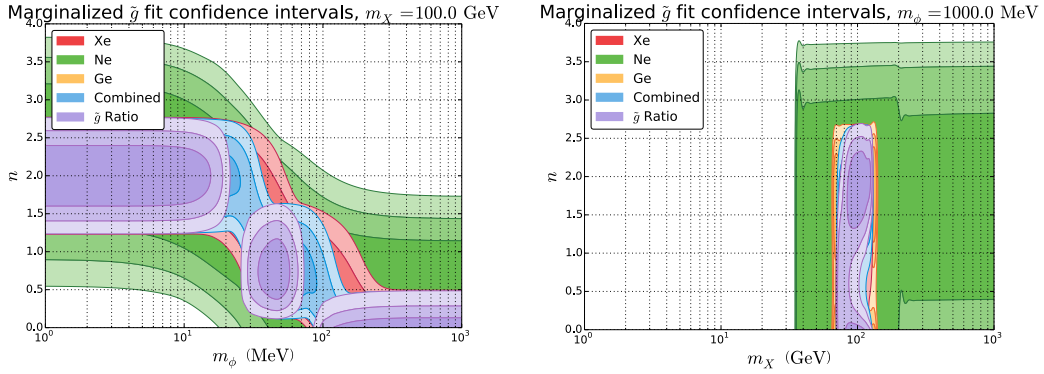


Figure 3. Reconstruction of DM parameters from an input spectrum generated via a massive mediator with q -independent cross section with $m_X = 100$ GeV.

which multiple experiments share observed events. Because the ratio test does not require any assumption of a velocity distribution, and therefore does not require the observer to find a best fit by varying DM velocity profile parameters, it is typically more than $\sim 10\times$ faster than performing a χ^2 analysis of the data.

As a first example, let us examine the results coming from the $m_X = 20$ GeV case with a massless mediator with $n = 0$. This would arise for example from the exchange of a light vector or scalar. The marginalised $(1, 2, 3)\sigma$ best-fit contours are displayed in both the (m_ϕ, m_X) and (n, m_X) planes in the upper panel of Fig. 2. There we see that in addition to the benefit of having multiple targets with signal data, we also observe the utility of the \tilde{g} ratio test as defined in Sec. 3. In this example, the DM mass is precisely determined, while the operator integer is constrained to be $n \lesssim 0.5$, and the mediator mass bounded to be $m_\phi \lesssim 10$ MeV. In this conservative example, we have shown that one can learn the DM mass while simultaneously learning that a new light force carrier connects DM and nuclei.

It is useful to know how general this conclusion is, and in particular if it holds for heavier DM. We simulate the situation of 10^3 GeV DM again interacting with a massless mediator and display the results in the bottom panel of Fig. 2. Here only a lower bound on the DM mass $m_X \gtrsim 450$ GeV is possible. This is a result of a well-known $m_X - \sigma_n$ degeneracy at high DM mass that has been previously observed in spin-independent scattering (see e.g. [11, 32]), and arises simply from the fact that v_{min} becomes independent of the DM mass at high m_X . Despite this degeneracy however both the mediator mass and operator integer remain well-constrained, $m_\phi \lesssim 70$ MeV, and $n \lesssim 0.4$ respectively.

As an example of possible degeneracies with our technique, we consider the possibility of inferring that DM-nucleon scattering contains no momentum dependence. An example of this sort with 100 GeV DM is shown in Fig. 3. Here we have chosen $n = 0$ and $m_\phi = 1$ GeV such that no relevant momentum dependence enters into the scattering cross section. There we observe that both the mass of the mediator and the operator integer n are not well-determined by the data. This is simply from the fact that a momentum-independent cross section could arise “accidentally” from the exchange of a light mediator with $n = 2$ such that the two types of momentum-dependence cancel each other out. In this case the DM mass can be reliably re-constructed while the operator which produces the DM-quark interaction is limited to a trio of pair-wise constraint (either $n = 0$ contact interaction, $n = 1$ with $m_\phi \approx 45$ MeV, or $n = 2$ with a masses mediator). Orthogonal data (e.g. collider or astrophysical) would be necessary to infer which class of DM microphysics is truly responsible for the interaction, but the total breadth of possible operators and mediators would now be more tightly constrained.

To illustrate the true halo independent character of the ratio test we have conducted an example where the χ^2 test was intentionally conducted under an incorrect assumption of the type of velocity distribution present in the DM halo. An initial data set was prepared using $n = 2$, $m_X = 500$ GeV, and $m_\phi = 100$ MeV with a SHM velocity profile with the parameters $\langle v_e(t) \rangle = 230$ km/s, $v_{esc} = 550$ km/s, $v_0 = 230$ km/s. The data was analyzed according to the χ^2 test as outlined above, with the exception that the Earth’s rotational velocity relative to the DM halo was set to 0 km/s. As a result isolated experiments (particularly Xenon) were able to obtain good individual fits to the original microphysics of the DM, but the Combined analysis of all observation fails to correctly reconstruct the properties of the DM, ruling out the true parameters with a confidence of $> 4\sigma$. In contrast, because the ratio test requires no assumption be made about the DM velocity distribution it is able to correctly identify the true DM interaction parameters as the best fit, along with the expected degeneracies between n and m_ϕ for a momentum dependent cross section discussed above.

Lastly it is important to note that many models of DM interactions yield terms in the cross section with disparate momentum dependence. A simple example of this is offered by both magnetic and electric dipole DM. Practically it is often the case that only one such

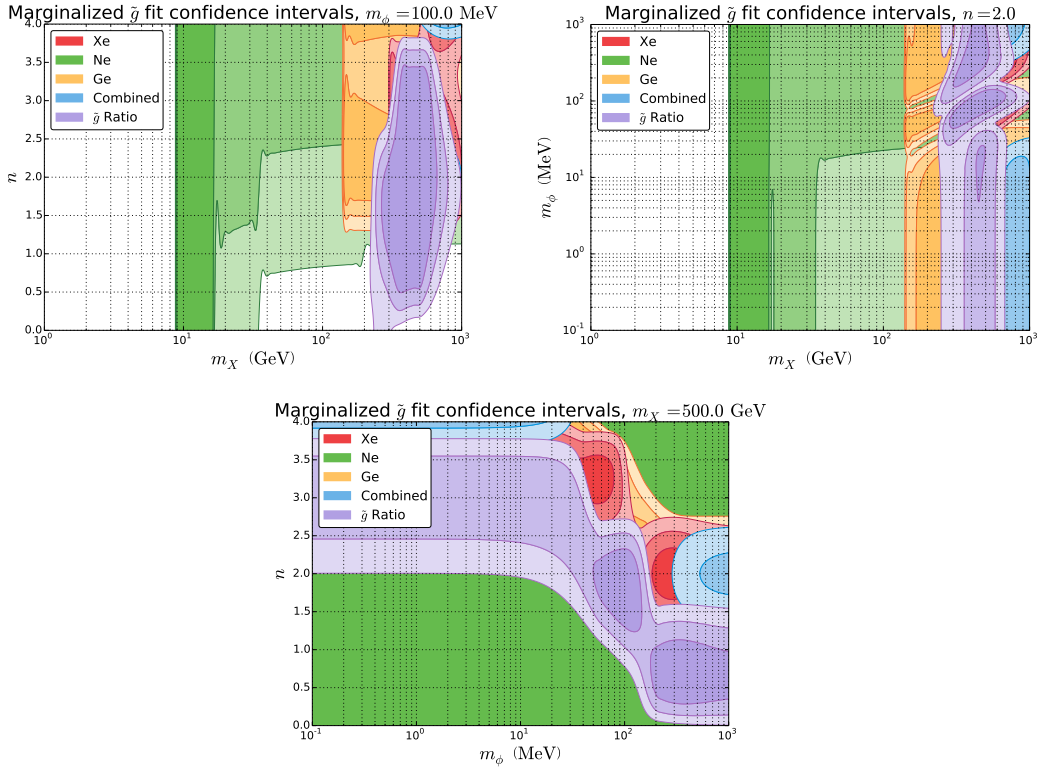


Figure 4. Reconstruction of DM parameters from an input spectrum generated with $n = 2$, $m_X = 500$ GeV, and $m_\phi = 100$ MeV. The initial data set was generated with a SHM velocity profile, but the χ^2 analysis was conducted under the assumption of a pure Maxwell-Boltzmann velocity distribution. Note that because of the incorrect choice of velocity distribution, the combined χ^2 analysis *rules out* the actual DM interaction parameters with a confidence of $> 4\sigma$.

term contributes significantly to the scattering rate. However even in the case that multiple terms with different q dependences enter, the method illustrated presently would yield a determination of some non-integer value of n . Beyond such a determination, we leave the extension of this method to more general momentum-dependence for future work.

6 Conclusion

We have presented and illustrated a new method for determining the momentum dependence of DM from direct detection data in a genuinely halo independent manner. In many cases the momentum dependence of the DM-nucleus scattering cross section can be well-determined from future direct detection data. The complementarity of targets aids significantly in this determination. Moreover, it is worth stressing again that this is one of the few properties of dark matter microphysics that can be extracted from near-term experiments in a manner that is independent of the DM velocity distribution. This does not hold for the velocity-dependence of the scattering, which is completely degenerate with the form of the velocity distribution and cannot be robustly determined.

As we have argued, one especially interesting application of these methods is their ability to reveal the existence of a new light force carrier between DM and nuclei. Such mediators

have been invoked both in the context of evading collider and direct detection limits while retaining a sufficiently large annihilation cross section to be a thermal relic. Moreover such mediators could be relevant for the self-scattering of DM [33–35].

Acknowledgements

The CP3-Origins centre is partially funded by the Danish National Research Foundation, grant number DNRF90. MTF acknowledges a Sapere Aude Grant no. 11-120829 from the Danish Council for Independent Research. This work was also supported in part by the U.C. Office of the President in conjunction with the LDRD Program at LANL.

A Signal Analysis

Now that we have established the basic ingredients which create a dark matter signal in our suite of next generation detectors, we must endeavor to determine what sort of information might be extracted from such a signal. We are primarily interested in extracting the momentum dependence n of the dark matter interaction with ordinary baryonic matter. It is also possible that one might extract the dark matter mass and the mass of the mediator which couples DM and quarks from the halo independent parameterization of $\tilde{g}(v_{min})$, in addition to the momentum dependence of the interaction.

A.1 Basic χ^2 Test

In order to compute the expected number of events for each experiment we must specify a velocity distribution. In this appendix, we outline our method for this by adopting the SHM and varying the velocity dispersion v_0 by $\pm 50\%$ to produce a best-fit to the data in our selected v_{min} bins. We follow the notation of [25] for the SHM where the dispersion, escape speed, and boost velocity from the Galactic to Earth frame are respectively v_0 , v_{esc} , and v_{obs} .

Once the simulated signal has been generated for a given detector (outlined in Section 4) our task turns to the business of constraining what range of parameters produces a good fit to the data. We choose to vary the momentum dependence, n , dark matter mass m_X , and the interaction mediator mass m_ϕ over the parameter space. Once we have chosen a given trio of n , m_X , and m_ϕ this allows us to normalize the overall dark matter cross section, σ_X , by scaling the predicted number of events to match total number of events in the simulated data set. This is possible because of the relative insensitivity of the shape of the function $\tilde{g}(v_{min})$ to the choice of v_{obs} , v_{esc} , and σ_v . The present observational uncertainty in these quantities is (by construction) not reflected in the overall normalization of $\tilde{g}(v_{min})$.

The normalization of the dark matter cross section is performed independently for each of the three detector media. Our intent to mimic the actions of independently operated detection experiments, which would reasonably choose to first analyze the data in their own detector as an isolated set of events.

Having generated an expected signal we then compare the simulated signal data $\{x_i\}$ for a given detector to the expected signal $\{\mu_i\}$ for fixed n and m_X . For the data within $\{x_i\}$ which contain at least 1 event in a single bin, we compute χ^2 in the usual fashion,

$$\chi^2 = \sum_i \frac{(x_i - \mu_i)^2}{\sigma_i^2}, \quad (\text{A.1})$$

where σ_i^2 is the variance of expected number of events μ_i under the assumption of gaussian random noise.

We must also include the contributions from bins which have few events, and are consequently dominated by Poisson noise. The remaining bins in $\{x_i\}$ which contain at less than 1 event are treated using the ‘‘Log Likelihood’’ method (also known as the ‘‘Product of Poissons’’ method). The Poisson probability, P_i , for each bin in the remaining data to match the expected number of events is,

$$P_i = \frac{\mu_i^{x_i}}{x_i!} e^{-\mu_i}. \quad (\text{A.2})$$

The Likelihood, L , of observing the signal $\{x_i\}$ in bins with low numbers of events is given by the product of the Poisson probabilities,

$$L = \prod_i P_i = \prod_i \frac{\mu_i^{x_i}}{x_i!} e^{-\mu_i}. \quad (\text{A.3})$$

In order to convert the Likelihood, L , into a χ^2 value, one equates L with the value of the χ^2 probability distribution function with k degrees of freedom,

$$L = \frac{1}{2^{k/2} \Gamma(k/2)} \chi_L^{k-2} e^{-\chi_L^2/2}, \quad (\text{A.4})$$

where k is the number of bins used in computing L , $\Gamma(t) = \int_0^\infty x^{t-1} e^{-x} dx$, and χ_L^2 is the χ^2 contribution from data bins with less than 5 events. While there is no general analytic solution for Equation A.4, it can be numerically evaluated for χ_L^2 , giving the total value, χ_{total}^2 , for the data set,

$$\chi_{total}^2 = \chi^2 + \chi_L^2. \quad (\text{A.5})$$

This allows us to compute the fit probability, P_{final} , for the expected signal generated by our choice of n and m_X from the cumulative distribution function of χ^2 for Poisson random variables,

$$P_{final}(m/2, \chi^2/2) = \frac{\Gamma(m/2, \chi^2/2)}{\Gamma(m/2)}, \quad (\text{A.6})$$

where m is the total number of degrees of freedom in the data set $\{x_i\}$, and $\Gamma(t, s) = \int_s^\infty x^{t-1} e^{-x} dx$, the upper incomplete gamma function.

In addition to evaluating the goodness of fit for the hypothetical Ne, Ge, and Xe detectors, we also evaluate the combined fit to all of the experimental data sets. This is done simply by repeating the steps outlined in Equations 12-17 for the combined data set $\{x_j^{combined}\} = \{\{x_i^{Ne}\}, \{x_i^{Ge}\}, \{x_i^{Xe}\}\}$, with the associated combined predicted number of events $\{\mu_j^{combined}\} = \{\{\mu_i^{Ne}\}, \{\mu_i^{Ge}\}, \{\mu_i^{Xe}\}\}$.

A.2 Ratio Test

There is an additional test which provides an improved diagnostic of the microphysics governing the dark matter nucleon interaction which is possible only when comparing two or more experiments which have distinct detection media. We begin by supposing that there is only a single species of dark matter which is detected by our suite of experiments. This is by no means a certainty, but for our purposes the introduction of multi-component dark matter would produce undue complexity which is not motivated by current observational constraints. With single component dark matter, we can say concretely that there can

be only one dark matter velocity distribution which is sampled by all of the experiments, $\tilde{g}_{true}(v_{min})$. However, in the instance that the momentum dependence of the dark matter interaction is a free parameter, the reconstructed function $\tilde{g}_{infer}(v_{min})$ is modified by both the reduced mass of the dark matter-nucleus system and the momentum dependence of the dark matter interaction, i.e. Equation 3.1. By proceeding bin by bin and comparing the overall normalization of $\tilde{g}_{infer}(v_{min})$ from detectors which employ different media, we can derive a constraint on the allowed ratio of $\tilde{g}_{infer}(v_{min})$ between the two experiments. One can choose to compare the ratio of $\tilde{g}_{infer,1}/\tilde{g}_{infer,2}$, which is shown in Equation 3.6, or to reconstruct $\tilde{g}_{true,1}(v_{min})/\tilde{g}_{true,2}(v_{min})$ under a chosen set of DM interaction parameters and verify that the ratio is equal to unity. Both of these techniques are equivalent and together they define what we call the ‘‘Ratio’’ test, wherein the reconstructed $\tilde{g}(v_{min})$ functions from multiple distinct experiments must satisfy the requirement that all experiments observe the same velocity distribution self-consistently.

To begin with we take the synthetic events, $\{x_i\}$, for each detector medium and re-bin them in v_{min} for a specific choice of m_X according to Equation 2.3. This reorganization ensures that the data sets for all of the experiments, $\{x_i^{Ne}\}, \{x_i^{Ge}\}, \{x_i^{Xe}\}$, share bins which sample identical regions of the velocity space. For each bin of the data sets which contains observed events, we obtain an inference of $\langle\tilde{g}(v_{min})\rangle$ within that bin by taking the average of Equation 2.4 over the bin width, $\Delta v_{min} = v_{min,f} - v_{min,i}$,

$$\begin{aligned} \langle\tilde{g}(v_{min})\rangle &= \frac{1}{\Delta v_{min}} \int_{v_{min,i}}^{v_{min,f}} \tilde{g}(v'_{min}) dv'_{min} \\ &= \frac{1}{\Delta v_{min}} \int_{v_{min,i}}^{v_{min,f}} \frac{2\mu_{nX}^2}{[f_p/f_n Z + (A - Z)]^2 F^2(E_R(v'_{min}))} \frac{dR}{dE_R(v'_{min})} dv'_{min}. \end{aligned} \quad (\text{A.7})$$

Whether one recovers $\langle\tilde{g}_{true}(v_{min})\rangle$ or $\langle\tilde{g}_{infer}(v_{min})\rangle$ from Equation A.8 depends on if the DM momentum dependent interaction physics included in $\frac{dR}{dE_R}$, or excluded, respectively. This result is subject to the overall normalization constraint that it must satisfy Equation 4.1 for the bin in $\{x_i\}$ we are treating.

Once the full set of data has been converted into a set of measured $\tilde{g}(v_{min})$, $\{\tilde{g}_i^{Ne}\}$, $\{\tilde{g}_i^{Ge}\}$, $\{\tilde{g}_i^{Xe}\}$, we can compute the ratio of \tilde{g} 's in overlapping v_{min} bins. We employ the assumption of Gaussian random noise in each bin to derive the statistical error associated with the computed ratio, which is then simply the addition in quadrature of the fractional error associated with each individual data bin in the ratio. This procedure produces a set of three ratio data sets $\{\{R_i^{Ne/Xe}\}, \{R_i^{Ne/Ge}\}, \{R_i^{Ge/Xe}\}\}$ and associated uncertainties $\{\{\sigma_i^{Ne/Xe}\}, \{\sigma_i^{Ne/Ge}\}, \{\sigma_i^{Ge/Xe}\}\}$. The expected values of these ratios, $\{\{\mu_i^{Ne/Xe}\}, \{\mu_i^{Ne/Ge}\}, \{\mu_i^{Ge/Xe}\}\}$, can be computed easily from Equation 3.6 if the \tilde{g}_{infer} ratio is used. If the \tilde{g}_{true} ratio is used, the expected value for all $\mu_i \equiv 1$. The χ^2 value of the ratio test is then computed directly from Equation A.1 for the entire data set, with the statistical significance following from Equation A.6.

References

- [1] M. Beltran, D. Hooper, E. W. Kolb, Z. A. Krusberg, and T. M. Tait, *Maverick dark matter at colliders*, *JHEP* **1009** (2010) 037, [[arXiv:1002.4137](#)].
- [2] J. Goodman, M. Ibe, A. Rajaraman, W. Shepherd, T. M. Tait, *et. al.*, *Constraints on Light Majorana dark Matter from Colliders*, *Phys.Lett.* **B695** (2011) 185–188, [[arXiv:1005.1286](#)].

- [3] Y. Bai, P. J. Fox, and R. Harnik, *The Tevatron at the Frontier of Dark Matter Direct Detection*, *JHEP* **1012** (2010) 048, [[arXiv:1005.3797](#)].
- [4] P. J. Fox, R. Harnik, J. Kopp, and Y. Tsai, *Missing Energy Signatures of Dark Matter at the LHC*, *Phys.Rev.* **D85** (2012) 056011, [[arXiv:1109.4398](#)].
- [5] M. Drees and C.-L. Shan, *Model-Independent Determination of the WIMP Mass from Direct Dark Matter Detection Data*, *JCAP* **0806** (2008) 012, [[arXiv:0803.4477](#)].
- [6] P. J. Fox, J. Liu, and N. Weiner, *Integrating Out Astrophysical Uncertainties*, *Phys.Rev.* **D83** (2011) 103514, [[arXiv:1011.1915](#)].
- [7] M. T. Frandsen, F. Kahlhoefer, C. McCabe, S. Sarkar, and K. Schmidt-Hoberg, *Resolving astrophysical uncertainties in dark matter direct detection*, *JCAP* **1201** (2012) 024, [[arXiv:1111.0292](#)].
- [8] E. Del Nobile, G. Gelmini, P. Gondolo, and J.-H. Huh, *Generalized Halo Independent Comparison of Direct Dark Matter Detection Data*, *JCAP* **1310** (2013) 048, [[arXiv:1306.5273](#)].
- [9] B. Feldstein and F. Kahlhoefer, *A new halo-independent approach to dark matter direct detection analysis*, [arXiv:1403.4606](#).
- [10] P. J. Fox, Y. Kahn, and M. McCullough, *Taking Halo-Independent Dark Matter Methods Out of the Bin*, [arXiv:1403.6830](#).
- [11] M. Pato, L. Baudis, G. Bertone, R. Ruiz de Austri, L. E. Strigari, *et. al.*, *Complementarity of Dark Matter Direct Detection Targets*, *Phys.Rev.* **D83** (2011) 083505, [[arXiv:1012.3458](#)].
- [12] M. Pato, L. E. Strigari, R. Trotta, and G. Bertone, *Taming astrophysical bias in direct dark matter searches*, *JCAP* **1302** (2013) 041, [[arXiv:1211.7063](#)].
- [13] S. D. McDermott, H.-B. Yu, and K. M. Zurek, *The Dark Matter Inverse Problem: Extracting Particle Physics from Scattering Events*, *Phys.Rev.* **D85** (2012) 123507, [[arXiv:1110.4281](#)].
- [14] P. J. Fox, G. D. Kribs, and T. M. Tait, *Interpreting Dark Matter Direct Detection Independently of the Local Velocity and Density Distribution*, *Phys.Rev.* **D83** (2011) 034007, [[arXiv:1011.1910](#)].
- [15] N. Bozorgnia, J. Herrero-Garcia, T. Schwetz, and J. Zupan, *Halo-independent methods for inelastic dark matter scattering*, *JCAP* **1307** (2013) 049, [[arXiv:1305.3575](#)].
- [16] G. Jungman, M. Kamionkowski, and K. Griest, *Supersymmetric dark matter*, *Phys.Rept.* **267** (1996) 195–373, [[hep-ph/9506380](#)].
- [17] S. Chang, A. Pierce, and N. Weiner, *Momentum Dependent Dark Matter Scattering*, *JCAP* **1001** (2010) 006, [[arXiv:0908.3192](#)].
- [18] M. T. Frandsen, F. Kahlhoefer, C. McCabe, S. Sarkar, and K. Schmidt-Hoberg, *The unbearable lightness of being: CDMS versus XENON*, *JCAP* **1307** (2013) 023, [[arXiv:1304.6066](#)].
- [19] V. Cirigliano, M. L. Graesser, and G. Ovanesyan, *WIMP-nucleus scattering in chiral effective theory*, *JHEP* **1210** (2012) 025, [[arXiv:1205.2695](#)].
- [20] V. Cirigliano, M. L. Graesser, G. Ovanesyan, and I. M. Shoemaker, *Shining LUX on Isospin-Violating Dark Matter Beyond Leading Order*, [arXiv:1311.5886](#).
- [21] A. Drukier, K. Freese, and D. Spergel, *Detecting Cold Dark Matter Candidates*, *Phys.Rev.* **D33** (1986) 3495–3508.
- [22] K. Freese, J. A. Frieman, and A. Gould, *Signal Modulation in Cold Dark Matter Detection*, *Phys.Rev.* **D37** (1988) 3388.
- [23] M. Kuhlen, N. Weiner, J. Diemand, P. Madau, B. Moore, *et. al.*, *Dark Matter Direct Detection with Non-Maxwellian Velocity Structure*, *JCAP* **1002** (2010) 030, [[arXiv:0912.2358](#)].

- [24] P. Smith and J. Lewin, *Dark Matter Detection*, *Phys.Rept.* **187** (1990) 203.
- [25] C. Savage, K. Freese, and P. Gondolo, *Annual Modulation of Dark Matter in the Presence of Streams*, *Phys.Rev.* **D74** (2006) 043531, [[astro-ph/0607121](#)].
- [26] C. McCabe, *The Astrophysical Uncertainties Of Dark Matter Direct Detection Experiments*, *Phys.Rev.* **D82** (2010) 023530, [[arXiv:1005.0579](#)].
- [27] J. Bovy, D. W. Hogg, and H.-W. Rix, *Galactic masers and the Milky Way circular velocity*, *Astrophys.J.* **704** (2009) 1704–1709, [[arXiv:0907.5423](#)].
- [28] P. J. McMillan and J. J. Binney, *The uncertainty in Galactic parameters*, [arXiv:0907.4685](#).
- [29] **LUX Collaboration** Collaboration, D. Akerib *et. al.*, *First results from the LUX dark matter experiment at the Sanford Underground Research Facility*, [arXiv:1310.8214](#).
- [30] M. T. Frandsen, F. Sannino, I. M. Shoemaker, and O. Svendsen, *LUX Constraints on Magnetic Dark Matter in the $S\bar{E}\chi\gamma$ Model with(out) Naturality*, [arXiv:1312.3326](#).
- [31] M. T. Frandsen and I. M. Shoemaker, *The Up-Shot of Inelastic Down-Scattering at CDMS-Si*, [arXiv:1401.0624](#).
- [32] A. Friedland and I. M. Shoemaker, *Integrating In Dark Matter Astrophysics at Direct Detection Experiments*, *Phys.Lett.* **B724** (2013) 183–191, [[arXiv:1212.4139](#)].
- [33] J. L. Feng, M. Kaplinghat, and H.-B. Yu, *Halo Shape and Relic Density Exclusions of Sommerfeld-Enhanced Dark Matter Explanations of Cosmic Ray Excesses*, *Phys.Rev.Lett.* **104** (2010) 151301, [[arXiv:0911.0422](#)].
- [34] A. Loeb and N. Weiner, *Cores in Dwarf Galaxies from Dark Matter with a Yukawa Potential*, *Phys.Rev.Lett.* **106** (2011) 171302, [[arXiv:1011.6374](#)].
- [35] S. Tulin, H.-B. Yu, and K. M. Zurek, *Beyond Collisionless Dark Matter: Particle Physics Dynamics for Dark Matter Halo Structure*, *Phys.Rev.* **D87** (2013) 115007, [[arXiv:1302.3898](#)].